

First-principles study of migration mechanisms and diffusion of carbon in GaN

This content has been downloaded from IOPscience. Please scroll down to see the full text.

2015 J. Phys.: Conf. Ser. 633 012143

(<http://iopscience.iop.org/1742-6596/633/1/012143>)

View [the table of contents for this issue](#), or go to the [journal homepage](#) for more

Download details:

IP Address: 131.84.11.215

This content was downloaded on 06/09/2017 at 15:15

Please note that [terms and conditions apply](#).

You may also be interested in:

[Electronic and magnetic properties GaN/MnN/GaN and MnN/GaN/MnN interlayers](#)

C Ortega López, G Casiano Jiménez and M J Espitia

[Indirect excitation of Eu³⁺ in GaN codoped with Mg and Eu](#)

M Yamaga, H Watanabe, M Kurahashi et al.

[Theoretical investigation of GaN carbon doped](#)

M J Espitia Rico, M G Moreno Armenta, J A Rodríguez et al.

[Growth of GaAs on Preferentially Etched GaAs Surfaces by Migration-Enhanced Epitaxy](#)

Minoru Kawashima and Yoshiji Horikoshi

[Application of GaN for photoelectrolysis of water](#)

M V Puzyk, A S Usikov, S Yu Kurin et al.

[Steady-state and high-frequency electron transport in GaN nanowires](#)

V V Koroteyev, V A Kochelap, S Vitusevich et al.

[High-field electron transport in GaN under crossed electric and magnetic fields](#)

V A Kochelap, V V Koroteyev, G I Syngayivska et al.

[Technology development for GaN based power microwave DHFET](#)

A N Alexeev, V P Chaly, D M Krasovitsky et al.

[Ion-beam synthesis of GaN in silicon](#)

V A Sergeev, D S Korolev, A N Mikhaylov et al.

First-principles study of migration mechanisms and diffusion of carbon in GaN

Alexandros Kyrtsos¹, Masahiko Matsubara² and Enrico Bellotti^{1,2}

¹ Division of Materials Science and Engineering, Boston University, 15 St Mary's, Boston, USA

² Department of Electrical and Computer Engineering, Boston University, 8 St Mary's, Boston, USA

E-mail: akyrtsos@bu.edu

Abstract. Carbon related defects are readily incorporated in GaN due to its abundance during growth both with MBE and CVD techniques. Employing first-principles calculations we compute the migration barrier of neutral carbon interstitials in the wurtzite GaN crystal. The Minimum Energy Path (MEP) and the migration barriers of these defects are obtained using the Nudged Elastic Band (NEB) method with the climbing image modification (CI-NEB). In addition, the Dimer method is used to verify the results. The results yield a quantitative description of carbon diffusion in the crystal allowing for the determination of the most probable migration paths.

1 Introduction

Efficient LED lighting has developed in recent years thanks to III/nitride semiconductors such as GaN [1]. In addition to optoelectronic applications such as blue/green LEDs, GaN and its related alloys are used in power electronics [2] as well as photovoltaic applications [3].

Defects, both point [4] and extended ones [5, 6], affect the electronic properties of devices. Among them, carbon is a relevant and easily incorporated defect in GaN. Defect related levels in the band-gap may be the source of radiative recombination centers, leading to below gap emission compromising the performance of the device. A typical example of such a level is centered around 2.2 – 2.3 eV and is often referred to as the yellow luminescence (YL) [7–10]. This YL band can be present for both undoped samples [11] and samples containing carbon impurities [12–14]. Recent studies suggest that carbon related defects are responsible for the YL band [7, 15].

Carbon is a common impurity both in molecular beam epitaxy (MBE) [16, 17] and metal organic chemical vapor deposition (MOCVD) [18]. In the former case, carbon can contaminate the material during air exposure in standard substrate loading procedures or at the beginning of regrowth. In MOCVD, carbon is part of the metal organic compounds used as source material for gallium. In addition, carbon can be found as a contaminant in the source gases or it can be etched off the susceptor that transfers heat to the substrate. Even though carbon defects have been intensively investigated in the past, the current understanding of the migration mechanisms of these defects in GaN is still incomplete.

The migration paths and barriers of carbon interstitials in GaN were investigated using density-functional theory (DFT) [19, 20] in conjunction with the climbing image nudged elastic



band method (CI-NEB) [21, 22]. Using the CI-NEB method we ensure that the calculated energy corresponds to the migration barrier for a given path. In addition, we get information about the atomic configuration in the saddle point.

2 Background

It is empirically observed that most diffusion processes in solids exhibit a temperature dependence described by an Arrhenius law

$$D = D_0 e^{-\frac{Q}{k_B T}}, \quad (1)$$

where D_0 is a temperature independent factor, Q is the activation energy for the atomic jump mechanism and $k_B T$ is the product of the Boltzmann constant with temperature.

Deviations from this equation may be caused by the existence of short circuiting diffusion paths such as dislocations and grain boundaries, multiple diffusion mechanisms and impurity effects [23].

The jump rate is characterized by an attempt frequency and a thermodynamic factor that dictates the probability of an attempt resulting in a successful jump.

$$\Gamma = \Gamma_0 e^{-\frac{\Delta G}{k_B T}}. \quad (2)$$

The attempt frequency, Γ_0 , can be obtained within harmonic transition state theory via the Vineyard equation [24], but often the Einstein or Debye frequency is used instead. ΔG represents the isothermal work associated with the motion of the particle from the initial to the final state.

3 Computational Details

3.1 Computational method

The calculations were performed with the vienna *ab initio* simulation package (VASP) [25] using the projector augmented wave (PAW) method [26, 27]. The generalized gradient approximation (GGA) in the parametrization by Perdew, Burke and Ernzerhof (PBE) [28] was used. The investigation of the lowest energy paths was performed using the CI-NEB method [21, 22] as well as the Dimer method [29] as implemented in VASP through the VTST-Tools by Henkelman, Jónsson and others [30].

The convergence of the size of the supercell was investigated using supercells of 64, 72, 96, 128 and 144 atoms. The 64-atom supercell is found to be inadequate to contain the deformations induced by the migration of carbon. The 72-atom supercell might be sufficient for certain migrations but not all. Thus, we chose the 96-atom supercell to be the safest and most efficient option at hand. The plane-wave energy cutoff was set at 450 eV and a Γ -centered $2 \times 2 \times 2$ k-point mesh is used for the sampling of the Brillouin zone. The atomic configurations were relaxed until the maximum force per atom was less than 5×10^{-3} eV/Å. In the case of the NEB calculations, the images were relaxed until the maximum force per atom was no more than 10^{-2} eV/Å.

The crystallographic parameters of the w-GaN we obtained from our calculations are $a = 3.211$ Å, $c/a = 1.629$ and $u = 0.377$, which are in good agreement with the experimental values $a = 3.189$ Å, $c/a = 1.626$ and $u = 0.377$ and consistent with previous DFT calculations [31]. The bandgap at the Γ point is 1.757 eV which underestimates the experimental value of 3.4 eV as expected from GGA.

The main sources of error in DFT calculations of point defects are the electrostatic and elastic interactions of the defect between neighboring supercells and the underestimation of the bandgap. Lany and Zunger [32] describe a number of methods to overcome these shortcomings of DFT. However, migration barriers, the main focus of the present work, are calculated as

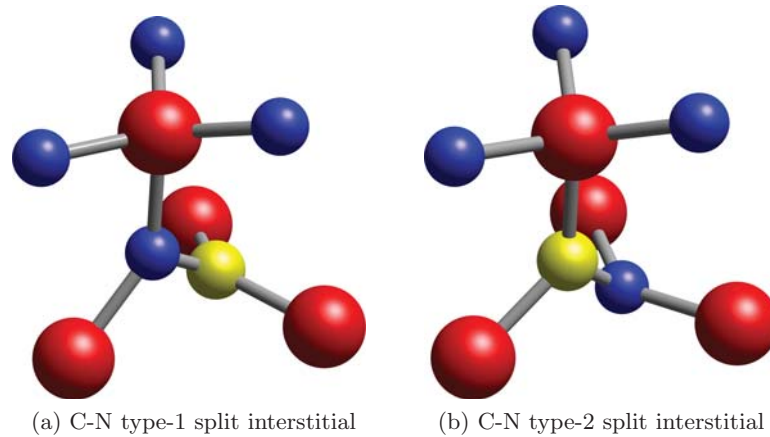


Figure 1: Split interstitials of carbon (yellow) and nitrogen (blue) surrounded by four gallium atoms (red).

energy differences of electronically similar configurations. Thus, there is no need to apply any correction scheme.

A typical systematic error in the formation energies calculations is considered to be approximately 0.1 eV [33]. Performing identical migrations at different sites we verified that the uncertainty of the migration barrier also lies within 0.1 eV.

In the NEB method [34], a set of “images” of the system is used to represent the migration path from the initial to the final configuration. The images (i.e., atomic configurations along the migration path) are connected with springs to resemble a string (or band). An optimization algorithm is then applied to relax the string down towards the minimum energy path. In the climbing image modification the highest energy image is driven to the saddle point by neutralizing the forces along the band. Since the image converges to the saddle point, the exact migration barrier can be calculated. In addition, the Dimer method was used to verify the saddle point location and the migration barrier acquired via the CI-NEB.

3.2 Determination of diffusion paths

The two most stable configurations for the neutral carbon interstitial are the type-1 and type-2 C-N split complexes shown in Fig. 1. They differ by less than 0.1 eV [35]. Hence, both cases are investigated as potential initial and final configurations for the diffusion of carbon.

This small energy difference and the similarity of the two configurations allows for migrations accompanied by transformation from one type to the other. In this case, the migration barrier is defined as the energy difference between the saddle point and the lowest energy configuration. As a result, the barrier in this case could be smaller by ~ 0.1 eV following the opposite direction of the reaction.

The migration paths investigated in the present work have components both parallel and perpendicular to the c-axis of the wurtzite crystal. The endpoints of the migrations are either a type-1 or type-2 split interstitial. Fig. 2 presents the different migration paths considering jumps among the first and second nearest neighbors. The different combinations of paths and endpoint configurations result in nine different calculations.

Process A, shown in Fig. 2 refers to motion between two out of plane first nearest neighbors. A single gallium atom forms four bonds with nitrogens in the ideal crystal. Three of these nitrogens lie on a plane which is perpendicular to the [0001] direction. Process A describes the migration of a carbon atom forming a split with one of these three nitrogens to the fourth

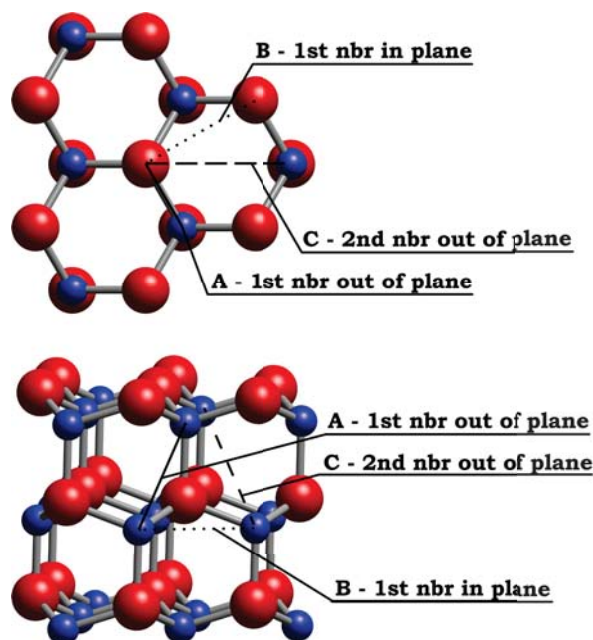


Figure 2: Diffusion paths available to carbon interstitial considering jumps among the first and second nearest neighbors.

nitrogen which is out of plane.

In the case of process B, migration occurs between two adjacent nitrogens lying on a plane perpendicular to the $[0001]$ direction. This process is a first nearest neighbor migration process and together with process A is expected to exhibit the lowest migration barriers.

As an additional process, we consider process C in which migration occurs between the second nearest neighbors which lie in different planes with respect to the $[0001]$ direction. Even though this process utilizes the hexagonal channel of the wurtzite structure, it is expected to exhibit the highest barriers since it is a second nearest neighbor migration.

4 Results

The difference of the formation energy between the two types of interstitials is 0.13 eV with the type-2 being the lowest in energy. The bond length between the carbon and the nitrogen is 1.29 Å and 1.31 Å for the type-1 and type-2 respectively.

The results obtained using the CI-NEB method are summarized in Table 1. The lowest migration barrier is observed in the case of process A from a type-2 interstitial to a type-1. This barrier becomes even smaller by approximately 0.1 eV if the reaction path is reversed. The diffusion potential energy along the reaction path is shown in Fig. 3.

The Dimer method verifies the results acquired by the CI-NEB for all the process A migrations. Both methods result in the same atomic configuration for the saddle point and consequently the same migration barrier. In the case of the lowest barrier migration, the saddle point lies closer to the type-1 interstitial. With respect to the straight line between the initial and final configurations, the saddle point forms an angle of 29° and 16° with the type-1 and type-2 ends respectively.

First nearest neighbor in plane migrations (process B) exhibit barriers close to 3 eV making them unfavorable compared to their out of plane counterparts. As expected, second nearest neighbor out of plane migrations require a much greater activation energy.

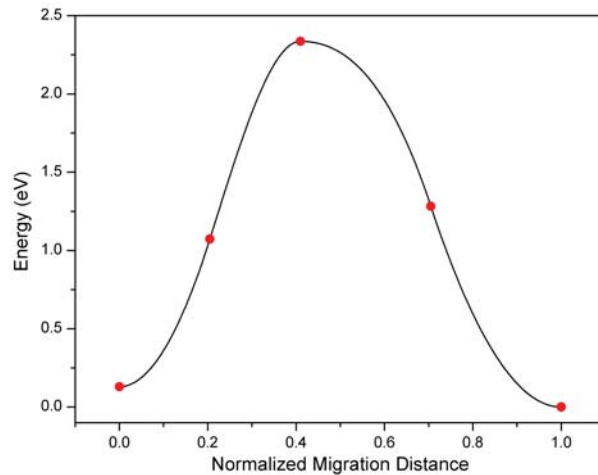


Figure 3: Diffusion energy barrier for a process A migration from a type-1 to type-2 split carbon interstitial.

Table 1: Energy barriers for carbon interstitial migration as obtained from CI-NEB calculations.

Migration Process	Initial	Final	Barrier (eV)
A	s1	s1	2.6
	s2	s2	2.7
	s1	s2	2.3
B	s1	s1	2.9
	s2	s2	3.1
	s1	s2	3.1
C	s1	s1	4.0
	s2	s2	—
	s1	s2	4.0

In order to estimate the temperature where carbon interstitials are activated we assume a jump rate of 1 Hz and a typical Debye frequency of 10 THz. Then, using eq. (2) and the calculated migration barriers, one can estimate the temperature where migration occurs. Hence, using $\Gamma = 1$ Hz, $\Gamma_0 = 10^{13}$ Hz and $\Delta G = 2.3$ eV we estimate that carbon interstitials are activated at temperatures close to 890 K. This temperature is relevant during growth of GaN both with MBE and CVD techniques.

5 Conclusions

We employed the Climbing Image Nudged Elastic Band technique to explore migration barriers of carbon diffusion in GaN. The Dimer method was also used in order to verify the results obtained by the CI-NEB in the case of the three lowest energy barrier migrations. The two most

stable interstitial types of carbon are investigated with respect to diffusion via first and second nearest neighbor mechanisms.

The first out of plane nearest neighbor mechanism exhibits the lowest migration barriers indicating a favorable direction of migration along the [0001] axis of the crystal. However, for growth temperatures, where carbon migration is relevant, the in plane migration is also competing. Migration via the second nearest neighbor mechanism exhibits high energy barriers minimizing the probability for this mechanism to contribute to the carbon diffusion.

Acknowledgments

The authors gratefully acknowledge financial support from the U.S. Army Research Laboratory through the Collaborative Research Alliance (CRA) for Multi-Scale multidisciplinary Modeling of Electronic Materials (MSME). The computational resources were provided by the 2014 ARO DURIP Award made to Dr. E. Bellotti.

References

- [1] Pimputkar S, Speck J S, DenBaars S P and Nakamura S 2009 *Nature Photonics* **3** 180–182
- [2] Mishra U K, Parikh P and Wu Y F 2002 *Proceedings of the IEEE* **90** 1022–1031
- [3] Dahal R, Li J, Aryal K, Lin J Y and Jiang H X 2010 *Applied Physics Letters* **97** 1–4
- [4] Limpijumnong S and Van de Walle C G 2004 *Phys. Rev. B* **69**(3) 035207
- [5] Matsubara M, Godet J, Pizzagalli L and Bellotti E 2013 *Applied Physics Letters* **103**
- [6] Matsubara M, Pizzagalli L and Bellotti E 2014 *physica status solidi (c)* **11** 521–524
- [7] Demchenko D O, Diallo I C and Reshchikov M A 2013 *Physical Review Letters* **110** 1–5
- [8] Suski T, Perlin P, Teisseyre H, Leszczynski M, Grzegory I, Jun J, Bockowski M, Porowski S and Moustakas T D 1995 *Applied Physics Letters* **67** 2188–2190
- [9] Reshchikov M A and Morkoç H 2005 *Journal of Applied Physics* **97**
- [10] Ogino T and Aoki M 1980 *Japanese Journal of Applied Physics* **19** 2395
- [11] Glaser E, Kennedy T and Doverspike K 1995 *Physical Review B* **51** 326–336
- [12] Kucheyev S O, Toth M, Phillips M R, Williams J S, Jagadish C and Li G 2002 *Journal of Applied Physics* **91** 5867–5874
- [13] Seager C H, Wright A F, Yu J and Götz W 2002 *Journal of Applied Physics* **92** 6553–6560
- [14] Armstrong A, Arehart A R, Green D, Mishra U K, Speck J S and Ringel S A 2005 *Journal of Applied Physics* **98**
- [15] Lyons J L, Janotti A and Van De Walle C G 2010 *Applied Physics Letters* **97** 5–7
- [16] Koblmüller G, Chu R M, Raman A, Mishra U K and Speck J S 2010 *Journal of Applied Physics* **107**
- [17] Ber B Y, Kudriavtsev Y A, Merkulov A V, Novikov S V, Lacklison D E, Orton J W, Cheng T S and Foxon C T 1998 *Semiconductor Science and Technology* **13** 71
- [18] Shah P B, Dedhia R H, Tompkins R P, Viveiros E A and Jones K A 2012 *Solid-State Electronics* **78** 121–126
- [19] Hohenberg P and Kohn W 1964 *Phys. Rev. B* **136**(3B) 864–871
- [20] Kohn W and Sham L J 1965 *Physical Review A* **140**
- [21] Henkelman G, Uberuaga B P and Jónsson H 2000 *Journal of Chemical Physics* **113** 9901–9904
- [22] Henkelman G and Jónsson H 2000 *The Journal of Chemical Physics* **113** 9978–9985

- [23] Swalin R A 1973 *Atomic Diffusion in Semiconductors* ed Shaw D (Springer US) chap 2, pp 65–110
- [24] Vineyard G H 1957 *Journal of Physics and Chemistry of Solids* **3** 121–127
- [25] Kresse G and Furthmüller J 1996 *Phys. Rev. B* **54**(16) 11169–11186
- [26] Blöchl P E 1994 *Phys. Rev. B* **50**(24) 17953–17979
- [27] Kresse G and Joubert D 1999 *Phys. Rev. B* **59**(3) 1758–1775
- [28] Perdew J P, Burke K and Ernzerhof M 1996 *Phys. Rev. Lett.* **77**(18) 3865–3868
- [29] Henkelman G and Jónsson H 1999 *The Journal of Chemical Physics* **111** 7010–7022
- [30] The Transition State Tools implementation for VASP can be obtained from <http://theory.cm.utexas.edu/vtsttools>
- [31] Stampfl C and Van de Walle C G 1999 *Phys. Rev. B* **59**(8) 5521–5535
- [32] Lany S and Zunger A 2008 *Phys. Rev. B* **78**(23) 235104
- [33] Zhang S B, Wei S H and Zunger A 2001 *Phys. Rev. B* **63**(7)
- [34] Jónsson H, Mills G and Jacobsen K W 1998 *Classical and quantum dynamics in condensed phase simulations* (World Scientific) chap 16, pp 385–404
- [35] Wright A F 2002 *Journal of Applied Physics* **92** 2575–2585